JOURNAL OF GEOPHYSICAL RESEARCH, VOL. 111, D23S14, doi:10.1029/2006JD007593, 2006

Observation of daytime N_2O_5 in the marine boundary layer during New England Air Quality Study–Intercontinental Transport and Chemical Transformation 2004

Hans D. Osthoff,[1,2] Roberto Sommariva,[1,2] Tahllee Baynard,[1,2] Anders Pettersson,[1,2] Eric J. Williams,[1,2] Brian M. Lerner,[1,2] James M. Roberts,[2] Harald Stark,[1,2] Paul D. Goldan,[1,2] William C. Kuster,[1,2] Timothy S. Bates,[3] Derek Coffman,[3] A. R. Ravishankara,[1,2,4] and Steven S. Brown[2]

Received 31 May 2006; revised 18 August 2006; accepted 11 October 2006; published 30 November 2006.

[1] The nitrate radical, NO_3, and dinitrogen pentoxide, N_2O_5, are key reactive nocturnal nitrogen oxides in the troposphere. The daytime impact of NO_3 and N_2O_5, however, is restricted by photochemical recycling of NO_3 to NO_2 and O_3. In this paper, we report daytime measurements of N_2O_5 on board the NOAA research vessel *Ronald H. Brown* in the Gulf of Maine during the New England Air Quality Study–Intercontinental Transport and Chemical Transformation (NEAQS-ITCT) campaign in the summer of 2004. Daytime N_2O_5 mixing ratios of up to 4 pptv were observed, consistent with predictions from a steady state analysis. Predicted and observed NO_3 mixing ratios were below the instrumental detection limit of ~1 pptv; the average calculated concentration was 0.09 pptv. Important impacts of daytime NO_3 and N_2O_5 in the marine boundary layer included increased rates of VOC oxidation (in particular dimethyl sulfide) and enhanced NO_x to HNO_3 conversion, both of which scaled with the available NO_x. Smaller effects of daytime NO_3 and N_2O_5 included chemical destruction of O_3 and a shift of the NO_2:NO ratio. Because the rates of heterogeneous conversion of N_2O_5 and NO_3 to HNO_3 scale with the surface area available for uptake, the importance of daytime fog is discussed.

Citation: Osthoff, H. D., et al. (2006), Observation of daytime N_2O_5 in the marine boundary layer during New England Air Quality Study–Intercontinental Transport and Chemical Transformation 2004, *J. Geophys. Res.*, *111*, D23S14, doi:10.1029/2006JD007593.

1. Introduction

[2] The nitrate radical, NO_3, and dinitrogen pentoxide, N_2O_5, have long been recognized as key reactive nighttime nitrogen oxides in the troposphere. For example, for certain VOCs the nitrate radical can be as important as a nocturnal oxidant as the hydroxyl radical, OH, is during the day [*Wayne et al.*, 1991]. In addition, heterogeneous uptake of N_2O_5 on aerosols [*Hu and Abbatt*, 1997; *Mozurkewich and Calvert*, 1988] and reaction of NO_3 with volatile organic compounds (VOCs) such as dimethyl sulfide (DMS) [*Butkovskaya and Lebras*, 1994; *Jensen et al.*, 1992; *Wallington et al.*, 1986] and aldehydes [*Atkinson*, 1991; *D'Anna et al.*, 2001] are efficient pathways for nighttime destruction of NO_x (= NO + NO_2), a key ingredient of photochemical ozone production [*Crutzen*, 1979]. The nitrate radical is produced by reaction of NO_2 with ozone; further reaction with NO_2 establishes a thermal equilibrium with N_2O_5.

$$NO_2 + O_3 \rightarrow NO_3 + O_2, k_1(298K) = 3.2 \times 10^{-17} cm^3 molecule^{-1} s^{-1} \quad (1)$$

$$NO_3 + NO_2 \leftrightarrow N_2O_5, K_{eq} = \frac{k_2}{k_{-2}} = 3.1 \times 10^{-11} cm^3 molecule^{-1} (298\ K) \quad (2)$$

[3] Even though the rate of NO_3 production via reaction (1) is not significantly altered between day and night, daytime concentrations of NO_3 and N_2O_5 are small because of reaction of NO_3 with NO, a predominantly daytime species, as well as NO_3 photolysis [*Johnston et al.*, 1996].

$$NO_3 + NO \rightarrow 2NO_2, k_3(298K) = 2.6 \times 10^{-11} cm^3 molecule^{-1} s^{-1} \quad (3)$$

$$NO_3 \xrightarrow{hv} NO_2 + O, j_{4a}, \phi_{NO_2} = 87\% \quad (4a)$$

$$NO_3 \xrightarrow{hv} NO + O_2, j_{4b}, \phi_{NO} = 13\% \quad (4b)$$

[1] Cooperate Institute for Research in Environmental Sciences, University of Colorado, Boulder, Colorado, USA.
[2] Chemical Sciences Division, Earth System Research Laboratory, NOAA, Boulder, Colorado, USA.
[3] Pacific Marine Environmental Laboratory, NOAA, Seattle, Washington, USA.
[4] Department of Chemistry and Biochemistry, University of Colorado, Boulder, Colorado, USA.

0148-0227/06/2006JD007593$09.00

Rate coefficients given above are from the NASA/JPL recommendation [*Sander et al.*, 2003].

[4] Under certain conditions, such as in urban air masses containing large quantities of O_3 and NO_x, small but nonnegligible concentrations of gas phase NO_3 and N_2O_5 can be sustained in the daytime. For example, Geyer and coworkers observed daytime NO_3 concentrations of up to 5 parts-per-trillion (pptv) by long-path differential optical absorption spectroscopy (DOAS) in polluted urban air near Houston, TX, 3 hours before sunset. Their analysis showed that reactions of NO_3 during the day can lead to loss of odd oxygen, or O_x ($\approx O_3 + NO_2$), and contribute to the oxidation of hydrocarbons such as monoterpenes [*Geyer et al.*, 2003].

[5] During the New England Air Quality Study–Intercontinental Transport and Chemical Transformation (NEAQS-ITCT) 2004, we measured NO_3 and N_2O_5 by cavity ring-down spectroscopy (CaRDS) from an aircraft platform (the NOAA WP-3) and observed several pptv of daytime N_2O_5 [*Brown et al.*, 2005]. In this paper, we present daytime in situ NO_3 and N_2O_5 measurements which were performed on board the NOAA research vessel *Ronald H. Brown* (R/V *Brown*) and compare the observed daytime NO_3 and N_2O_5 concentrations to what is expected from steady state calculations. The chief differences between the aircraft and ship data sets were the nature and magnitude of the chemical sinks for NO_3 and N_2O_5, which tended to be larger at the surface because of the presence of DMS, sea salt aerosol, and marine fog, among other reasons. In this paper, we discuss the implications of daytime NO_3 and N_2O_5 in the marine boundary layer, including (1) oxidation of VOCs such as DMS and α-pinene, (2) increased rate of $NO_x \rightarrow HNO_3$ conversion via heterogeneous hydrolysis on aerosol particles and fog droplets, (3) chlorine activation on sea salt aerosol, (4) accelerated loss of O_3, and (5) perturbation of the NO_2:NO ratio.

2. Campaign and Measurement Techniques

[6] An overview of the NEAQS-ITCT 2004 campaign is given by *Fehsenfeld et al.*, [2006]. R/V *Brown* sampled in the Gulf of Maine for six weeks and encountered a variety of conditions, including clean marine air, fog, and continental outflow containing NO_x, and anthropogenic and biogenic VOCs. To study the chemical evolution of such continental pollution plumes during transport within the marine boundary layer in the Gulf of Maine, R/V *Brown* carried instruments for the characterization of gas phase compounds and aerosols. Of particular interest to this work are a GC-MS for VOC measurements [*Goldan et al.*, 2004], a GC for speciated peroxycarboxylic nitric anhydride (PAN) measurements [*Roberts et al.*, 1998], chemiluminescence detectors for NO, NO_2, O_3, and total reactive nitrogen oxides (NO_y) [*Williams et al.*, 1998], filter radiometers for photolysis rates of NO_3 and NO_2, $j(NO_3)$ and $j(NO_2)$ (H. Stark et al., Atmospheric in situ measurement of nitrate radical (NO_3) and other photolysis rates using spectro- and filter radiometry, submitted to *Journal of Geophysical Research*, 2006, hereinafter referred to as Stark et al., submitted manuscript, 2006), and a cavity ring-down spectrometer for NO_3, N_2O_5, and NO_2 detection. The aerosol surface area was determined using particle number and size distributions measured from a differential mobility particle sizer (DMPS) and an aerodynamic particle sizer (APS) as described by *Bates et al.* [2005]. Inlets were located between 15 m and 18 m above sea level, forward of the exhaust stacks to prevent sampling the vessel's exhaust plume.

[7] Detection of NO_3 and N_2O_5 by CaRDS has been described in detail elsewhere [*Dubé et al.*, 2006], and only a brief description, along with details specific to the daytime measurements of NO_3 and N_2O_5 with this instrument, will be given here. In our CaRDS instruments, the nitrate radical is detected by absorption near its maximum at 662 nm ($\sigma_{NO_3} = 2.23 \times 10^{-17}$ cm^2 molecule^{-1} [*Yokelson et al.*, 1994]), and the concentration of N_2O_5 is determined from the increase of the 662 nm absorption signal following thermal conversion of N_2O_5 to NO_3 in a heated channel. The sample flow is filtered to remove particles. The instrument is zeroed by addition of $\sim$25 ppbv nitric oxide to the sample flow to chemically destroy NO_3 via reaction (3).

[8] The CaRDS NO_3 and N_2O_5 measurements have to be corrected for losses of NO_3 on the aerosol filter and walls of the PFA Teflon inlet, which often limit the accuracy of the measurements. On R/V *Brown*, inlet losses were minimized by replacing the sample line every 48 hours and the Teflon filter at least once per hour. The transmission efficiency of the inlet was $\sim$65% for NO_3 and $\sim$90% for N_2O_5 [*Dubé et al.*, 2006]. The 2 σ, 1 s, detection limit of the ring-down spectrometer employed on R/V *Brown* was $\sim$2 pptv for both NO_3 and N_2O_5. Because the detection limit was determined by both the baseline precision and the uncertainty of a variable baseline offset (see below) it did not significantly improve upon signal averaging. Data presented in this manuscript were averaged to 5 min.

[9] During daytime, the instrument suffered from several potential measurement artifacts. A zero offset arose from the change in NO_2 concentration ($\sigma_{NO_2}(662\text{ nm}) = 2.8 \times 10^{-21}$ cm^2 molecule^{-1} [*Voigt et al.*, 2002]) between signal and zero because of oxidation of a small amount of the added NO by ambient O_3 and NO_3. This effect was equivalent to NO_3 and N_2O_5 mixing ratios of about 0.05 pptv and 0.2 pptv, respectively. Furthermore, reading a zero using NO during the day shifts the existing NO_3 concentration, already in steady state with ambient NO (see below), to smaller values but not necessarily completely to zero. Measurement of N_2O_5 by thermal conversion to NO_3 is also affected by ambient NO, since the NO_3 produced in the thermolysis will be lost to reaction with NO. This produces a variable correction of up to 35% which depends on the ambient NO concentration [*Brown et al.*, 2005]. Because we have not attempted to correct for these effects, daytime NO_3 and N_2O_5 concentrations reported in this manuscript are lower limits.

[10] Finally, data acquired during NEAQS-ITCT 2004 on both the WP-3 and R/V *Brown* suggest that there was a small and variable daytime interference in the 662 nm absorption signal in the heated channel (discussed further in section 4).

3. Predicted Daytime Concentrations of NO_3 and N_2O_5

[11] In the troposphere during the summer, the daytime mixing ratios of NO_3 and N_2O_5 can be calculated to

reasonable accuracy from steady state expressions [*Brown et al.*, 2005; *Geyer et al.*, 2003]. The effects described in this manuscript are relevant to warm conditions ($T_{avg} = 18 \pm 3$ C) under which the thermal equilibrium between N_2O_5 and NO_3 is established rapidly, and the ratio of N_2O_5 to NO_3 is modest. For example, this ratio was approximately 4:1 for the average level of 2.2 ppbv of daytime NO_2 and the average 18 C air temperature of this data set, which was buffered by the sea surface temperature.

[12] In addition to reactions (3) and (4), NO_3 and N_2O_5 are removed from the atmosphere by heterogeneous processes as well as reactions of NO_3 with VOCs.

$$NO_3 \xrightarrow{VOC_i} \text{products}, k_5 = \sum_i \left(k_{VOC,i}[VOC]_i\right) \quad (5)$$

$$N_2O_5 \xrightarrow{het.} 2HNO_3, k_6 = \frac{1}{4} c_{N_2O_5} \gamma_{N_2O_5} S_{aerosol} \quad (6)$$

$$NO_3 \xrightarrow{het.} \text{products}, k_7 = \frac{1}{4} c_{NO_3} \gamma_{NO_3} S_{aerosol} \quad (7)$$

$k_{VOC,i}$ is the bimolecular rate coefficient for the reaction of the *i*th VOC with NO_3, $S_{aerosol}$ is the aerosol surface density (μm^2 cm^{-3}), $\gamma_{N_2O_5}$ (γ_{NO_3}) is the uptake coefficient of N_2O_5 (NO_3) on aerosol, and $c_{N_2O_5}$ (c_{NO_3}) is the mean molecular speed of N_2O_5 (NO_3) calculated from gas kinetic theory (at 298 K, c = 240, 320 m s^{-1} for N_2O_5, NO_3, respectively). For simplicity and consistency with previous analyses [e.g., *Aldener et al.*, 2006], $\gamma_{N_2O_5}$ was set to 0.03 independent of aerosol composition on the basis of laboratory parameterizations of N_2O_5 uptake on sulfate and ammonium sulfate aerosols over the relative humidity range encountered in this study (range 40–100%, median 92%). Surface deposition of NO_3 and N_2O_5 and heterogeneous uptake of NO_3 in the absence of fog were negligibly small. Heterogeneous uptake of NO_3,with an uptake coefficient $\gamma(NO_3) = 2 \times 10^{-4}$ [*Rudich et al.*, 1998], was important only in fog (see section 5.2.1), where NO_3 is believed to convert to NO_3^- by electron transfer reactions [*Rudich et al.*, 1998].

[13] During the daytime, NO_3 and N_2O_5 are in steady state with respect to their production from reaction (1) and (2), and loss via reactions (3)–(7) [*Brown et al.*, 2005]. In the absence of fog (see section 5.2.2), daytime concentrations of NO_3 and N_2O_5 were calculated from

$$[NO_3]_{calc} = \frac{k_1[NO_2][O_3]}{k_3[NO] + j_4 + k_5 + k_6K_{eq}[NO_2] + k_7} \quad (8)$$

and

$$[N_2O_5]_{calc} = K_{eq}[NO_2][NO_3]_{calc}. \quad (9)$$

More sophisticated calculations based on the Master Chemical Mechanism (MCM) model [*Carslaw et al.*, 1999a; *Jenkin et al.*, 2003; *Saunders et al.*, 2003] confirmed the accuracy of the above analytical expressions derived from the steady state calculations (R. Sommariva et al., manuscript in preparation, 2006).

4. Measured Daytime NO_3 and N_2O_5 in the Marine Boundary Layer

[14] The daytime mixing ratios of NO_3 in the entire R/V *Brown* data set were uniformly below the CaRDS detection limit, while daytime N_2O_5 signals were observed frequently. The largest observed daytime N_2O_5 mixing ratio not attributed to interferences was 4 pptv. These data were not corrected for potential systematic instrumental biases such as zeroing offsets (up to −0.20 pptv in the case of N_2O_5) and reactive loss of NO_3, generated from thermal conversion of N_2O_5, with ambient NO. The predicted average values from the steady state calculation were $[NO_3]_{calc,avg}$ = 0.09 pptv and $[N_2O_5]_{calc,avg}$ = 0.32 pptv.

[15] Daytime N_2O_5 signals were usually observed when R/V *Brown* sampled continental outflow in close proximity to the coast, for example on 29 and 30 July (Figure 1). Shown in Figure 2 are time series of data collected on 30 July. The air mass encountered on 30 July contained fresh urban emissions, evident from the large and variable NO_2 signal. The toluene to benzene ratio, which can be used as a photochemical clock because toluene is oxidized more rapidly by OH than benzene [*Roberts et al.*, 1984], was 2.0 ± 0.3 to 1, which corresponds to a photochemical age of 11 ± 3 hours [*de Gouw et al.*, 2005]. The NO_3 photolysis rate at this time was variable (between 0.1 s^{-1} and 0.2 s^{-1}), consistent with the presence of scattered cloud cover. The large NO_2 mixing ratio (about 15 ppbv) in the early part of Figure 2 shifted equilibrium (2) to the right, favoring N_2O_5 formation. Observed and modeled N_2O_5 mixing ratios at this time were ~1 pptv. In the afternoon (after 1700 UTC, or 1300 local time (LT)), R/V *Brown* sailed north and then east and intercepted a NO_x-rich plume, originating from the greater Boston area. Up to 3 pptv of N_2O_5 were observed at this time, in agreement with predictions from steady state. In the late afternoon (after 2000 UTC), R/V *Brown* encountered a NO_x-depleted but O_3-rich air mass. The toluene to benzene ratio (0.4 ± 0.1) was consistent with a photochemical age of two days. This plume contained emissions from the greater New York area, which was corroborated by a Lagrangian particle dispersion model (FLEXPART [*Stohl et al.*, 2005]) of the air mass history and an analysis of the PPN/PAN ratio (J. M. Roberts et al., private communication, 2006). The low NO_2 abundance shifted equilibrium (2) toward NO_3 and NO_2, such that the calculated N_2O_5 and NO_3 mixing ratios were ~0.25 pptv, below the instrumental detection limit.

[16] Midday 662 nm extinction signals in the heated (N_2O_5) channel in excess of the predicted steady state N_2O_5 mixing ratios were occasionally observed in both the WP-3 aircraft data set [*Brown et al.*, 2005] and intermittently in the ship based measurements. For example, on 29 July at 1700 UTC, the observed 662 nm absorption signal in the heated channel was significantly larger, by about a factor of two, than the predicted N_2O_5 steady state mixing ratio (Figure 3). The steady state expression is unlikely to significantly overestimate the NO_3 loss rate (i.e., the denominator of equation (8)) or underestimate the NO_3 production rate (i.e., the numerator of equation (8)) and thus underpredict the

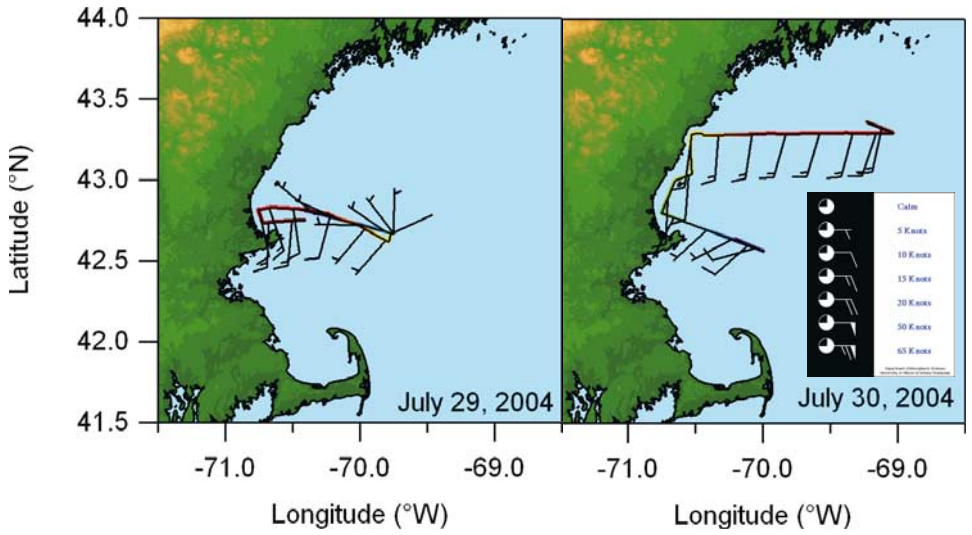

Figure 1. Ship location and wind direction on two sample days, during which N_2O_5 was observed in the daytime. On both days, R/V *Brown* sampled south-southwesterly air flow containing recent continental emissions north of Cape Anne along the Massachusetts and New Hampshire coasts in the northeastern United States.

observed concentrations. Therefore the excess signal in Figure 3 above the N_2O_5 steady state calculation was most likely a measurement artifact. On 29 July, the artifact correlated weakly with the mixing ratio of PAN (e.g., time series in Figure 3, in particular between 1600 and 1900 UTC); in other instances, however, there was no correlation between PAN and the difference between calculated and observed N_2O_5 signals (e.g., time series in Figure 2). Follow-up laboratory experiments, in which PAN, MPAN or HNO_3 from laboratory sources were added to the heated inlet, failed to produce a 662 nm absorption signal. At the present time, the origin of the apparent artifact observed in some of the daytime NEAQS-ITCT field data is unclear. One possible explanation is thermal dissociation of an unidentified gas phase species, possibly an organic nitrate or pernitrate, that is formed under conditions conducive to the formation of PAN (i.e., in sunlight), and that dissociates in the heated inlet to NO_3. We are currently investigating the source of the artifact.

5. Implications of Daytime NO_3 and N_2O_5 in the Marine Boundary Layer

[17] The observation of daytime N_2O_5 in the marine boundary layer implies that NO_3 and N_2O_5 have long enough atmospheric lifetimes for gas phase and heterogeneous reactions (other than reactions (3) and (4)) to occur. Further, the N_2O_5 observations in the absence of the artifact have corroborated the calculated, steady state concentrations in the present and the aircraft data set [*Brown et al.*, 2005]. Because N_2O_5 was frequently unmeasureable, we have also used steady state mixing ratios of NO_3 and N_2O_5 calculated from equations (8) and (9) to illustrate several aspects of daytime NO_3 and N_2O_5 in the polluted marine boundary layer. These include (1) enhanced daytime oxidation of VOCs (section 5.1), (2) heterogeneous uptake of N_2O_5 and NO_3 (section 5.2), (3) chemical ozone destruction, and (4) perturbation of the NO_2:NO ratio (section 5.3).

5.1. Increased Daytime Oxidation of VOCs by NO_3

[18] In the marine boundary layer, daytime oxidants include the hydroxyl radical (OH), ozone, halogens, and halogen oxides such as BrO, ClO, and IO [*Platt and Honninger*, 2003]. Although oxidation by halogens and halogen oxides may be significant in some instances, their contribution is neglected for the purpose of this specific analysis. The mixing ratios of OH, hydroperoxy radical (HO_2) and organic peroxy radicals (RO_2) were calculated using the Master Chemical Mechanism (MCM) [*Carslaw et al.*, 1999a, 1999b; *Jenkin et al.*, 2003; *Saunders et al.*, 2003]. Details of the calculation will be published elsewhere (R. Sommariva et al., manuscript in preparation, 2006). The average calculated OH and NO_3 mixing ratios between 0900 and 1500 LT (solar zenith angle $< 45°$) were 4.8×10^6 molecules cm^{-3} (0.19 pptv, 0.25 pptv at noon) and 1.9×10^6 molecules cm^{-3} (0.08 pptv). Thus the calculated midday mixing ratios of OH and NO_3 were approximately of the same order of magnitude. Typical midday OH mixing ratios varied from 5×10^6 to 2×10^7 molecules cm^{-3}, whereas calculated NO_3 mixing ratios ranged from 2×10^5 to 8×10^6 molecules cm^{-3}.

[19] Shown in Table 1 are rate coefficients for reactions of selected VOCs with OH, NO_3 and O_3. Shown in Table 2 are campaign averaged sets of mixing ratios of NO_3, OH, O_3, and NO_x as functions of NO_3 photolysis rates. From these, fractional VOC loss rates due to NO_3 oxidation, $f_{NO_3}(i)$, i.e., the relative amount of oxidation attributable to NO_3 for a particular VOC, were calculated.

$$f_{NO_3}(i) = \frac{k_{NO_3}(i)[NO_3]}{k_{NO_3}(i)[NO_3] + k_{OH}(i)[OH] + k_{O_3}(i)[O_3]} \quad (10)$$

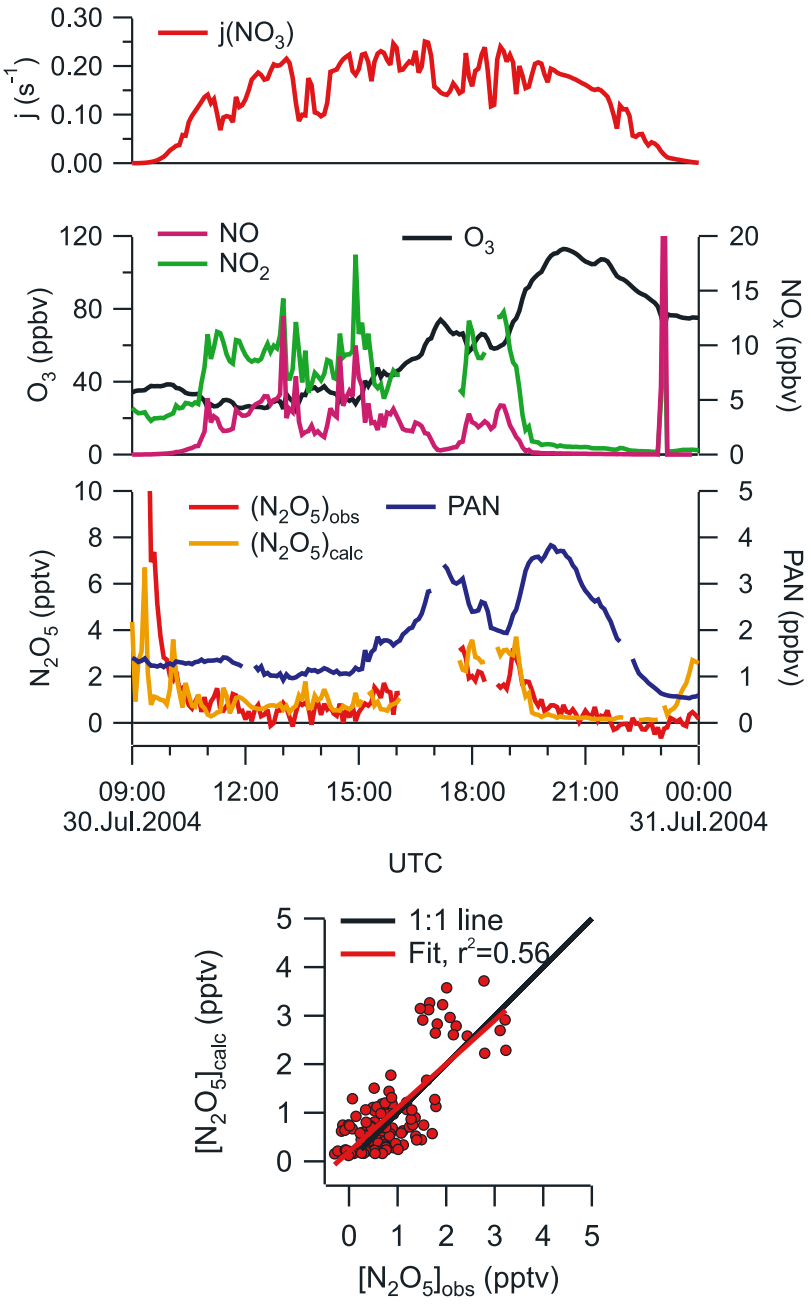

Figure 2. Example of a daytime N_2O_5 measurement. Data were averaged to 5 min. On 30 July, sunrise and sunset occurred at 0930 and 2400 UTC, respectively. There was broken cloud cover, which is evident in the $j(NO_3)$ time series (first panel). In the presence of 20 ppbv total NO_x and 40 ppbv O_3 (second panel), an N_2O_5 signal up to 3 pptv was observed (third panel). The concentration of NO_3 was below the instrumental detection limit. Observed N_2O_5 mixing ratios were not well correlated with PAN and were consistent with predicted values from a steady state calculation (fourth panel).

The data in Table 2 show that the amount of VOC oxidation attributable to NO_3 was, in general, small under clear sky conditions, but were larger for some VOCs (e.g., DMS).

[20] The campaign averages did not capture the NO_x scaling of daytime NO_3-driven VOC oxidation, which lead to significantly larger effects within NO_x-rich plumes. 30 July 2004, provides such an example, with NO_2 mixing ratios up to 15 ppbv. Although NO_3 was not measurable, its calculated concentration was in the range of 0.1 to 0.3 pptv (Figure 4, first panel), larger than the calculated OH concentrations (Figure 4, second panel). The presence of daytime NO_3 was corroborated by the observation of up to 3 pptv of daytime N_2O_5, in agreement with steady state (Figure 2). Concentrations of selected VOCs are plotted in the third panel of Figure 4. Dimethyl sulfide was observed in concentrations between 50 pptv close to the coast and 300 pptv further east (Figure 1). Between 1300 and 1400 UTC (0900–1000 LT), R/V *Brown* crossed a continental plume near the coast containing small amounts of isoprene and α-pinene. Shown in the fourth panel of Figure 4 are

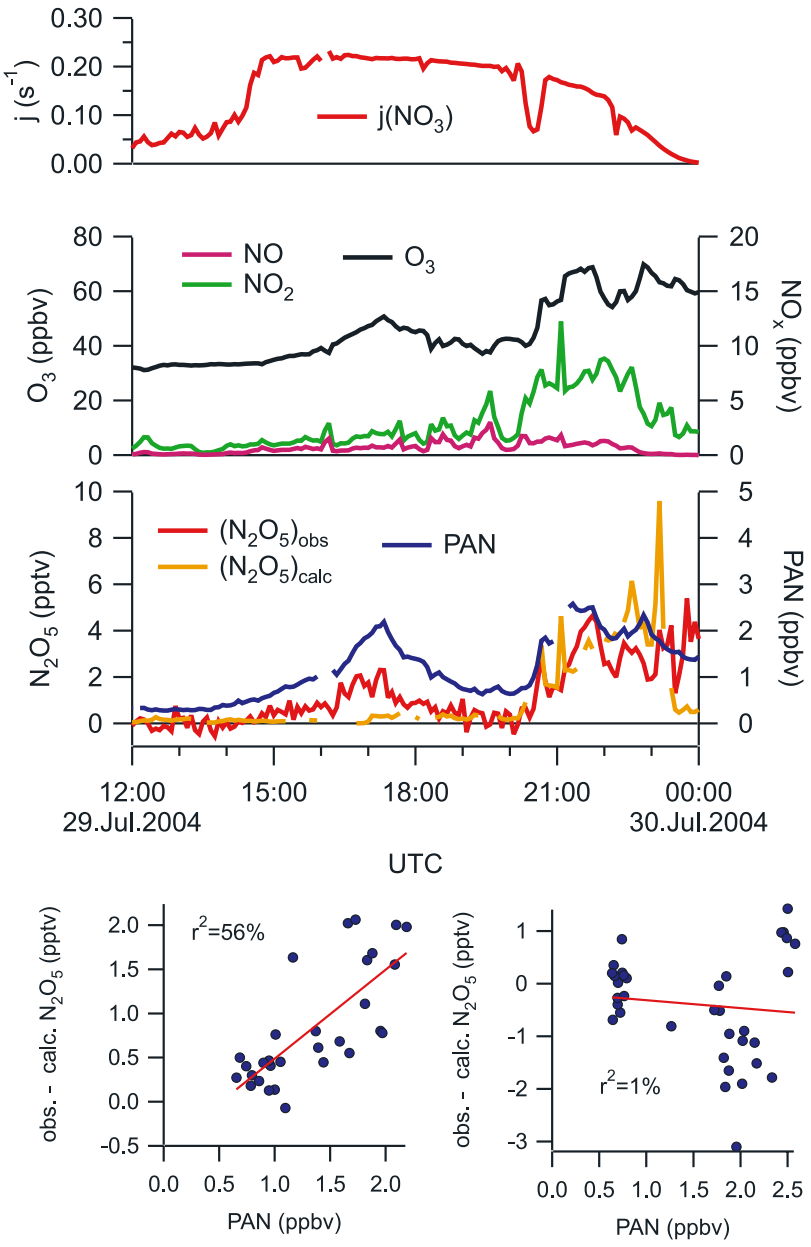

Figure 3. Example of a daytime measurement artifact. On 29 July around 1700 UTC, there was a 662 nm absorption signal in the heated channel that correlated with PAN that was not reproduced by steady state calculations. However, at 2100 UTC, with similar PAN mixing ratio, the observed N_2O_5 signals were reproduced by steady state calculations. Shown at the bottom are plots of the difference between the observed and calculated mixing ratio of N_2O_5 against PAN.

calculated fractional VOC loss rates due to NO_3 oxidation, f_{NO_3} (*i*) (equation (10)). In this example, about 15% of α-pinene observed in the continental plume before noon were oxidized by NO_3. In the afternoon (after 1800 UTC), the air mass no longer contained measurable α-pinene, likely because most of the α-pinene had been oxidized prior to the arrival of the continental air mass at the ship. Importantly, predicted daytime NO_3 oxidation of DMS within the high-NO_x air mass was comparable to that of OH throughout the day, with a peak value of 40% for f_{NO_3} (DMS).

[21] Figure 5 shows the scaling of f_{NO_3} (DMS) with NO_2 over a range from 0 to 5 ppbv, smaller than in the example of Figure 4 but encompassing the majority of the data from the campaign. Under midday, clear sky conditions, 5–15% of DMS oxidation was attributable to NO_3. Under lower-light conditions, however, NO_3 driven DMS-oxidation became comparable to or larger than OH oxidation for NO_2 levels greater than 2 ppbv at the ozone levels encountered during this campaign.

[22] There were three distinct classes of VOC whose oxidation rates were affected to some extent by the presence of daytime NO_3. These included DMS, terrestrially emitted biogenic VOC and their oxidation products, and certain highly reactive anthropogenic VOC. Daytime NO_3 oxidation of each class of VOC has a slightly different impact. For example, since the oxidation of DMS by NO_3 proceeds

Table 1. Reaction Rate Coefficients [*Atkinson*, 1990; *Atkinson and Arey*, 2003; *Atkinson et al.*, 1999; *Sander et al.*, 2003; *Wayne et al.*, 1991] for Reactions of Selected VOCs With OH, NO_3 and O_3[a]

Molecule	k_{OH}	k_{NO_3}	k_{O_3}	k_{OH}/k_{NO_3}
Ethane	2.5×10^{-13}	1.4×10^{-18}	$< 10^{-23}$	1.8×10^{5}
Ethylene	8.75×10^{-12}	2.1×10^{-16}	1.6×10^{-18}	4.2×10^{4}
Acetylene	4.6×10^{-13}	4.9×10^{-17}	1.0×10^{-20}	9.4×10^{3}
Methanol	9.3×10^{-13}	1.3×10^{-16}	–	7.2×10^{3}
CH_3SCH_3 (DMS)	5.0×10^{-12}	1.0×10^{-12}	$< 10^{-18}$	5
α-pinene	5.4×10^{-11}	6.2×10^{-12}	8.4×10^{-17}	9
Acetaldehyde	1.6×10^{-11}	2.8×10^{-15}	6×10^{-21}	6.0×10^{3}
Isoprene	$>1.0 \times 10^{-10}$	6.8×10^{-13}	1.3×10^{-17}	140
Methyl vinyl ketone	2.2×10^{-11}	4.7×10^{-16}	5.4×10^{-18}	4.7×10^{4}
Methacrolein	2.8×10^{-11}	3.7×10^{-15}	1.2×10^{-18}	7.6×10^{3}
3-methyl furan	9.4×10^{-11}	1.3×10^{-11}	2.0×10^{-17}	7
Benzene	1.25×10^{-12}	3×10^{-17}	2×10^{-22}	4.2×10^{4}
Toluene	5.7×10^{-12}	6.8×10^{-18}	4.5×10^{-22}	8.4×10^{5}
Styrene	1.1×10^{-10}	4.7×10^{-12}	1.7×10^{-17}	20
o-cresol	3.3×10^{-11}	1.2×10^{-11}	1.9×10^{-19}	3
m-cresol	6.8×10^{-11}	9.7×10^{-12}	1.9×10^{-19}	7
Phenol	2.8×10^{-11}	5.9×10^{-12}	–	5

[a]Unit is cm^3 $molecule^{-1}$ s^{-1}. VOCs were selected either on the basis of their abundance in the New England marine boundary layer (e.g., small hydrocarbons and oxygenates), or their reactivity with NO_3 (e.g., styrene and the phenols). Since NO_3 is known to be an important oxidant for biogenic VOC and DMS, selected biogenic VOC and some of their photochemical oxidation products have also been included. All rate coefficients are at 298 K.

exclusively by hydrogen abstraction [*Jensen et al.*, 1992] and the oxidation by OH can proceed by either addition (25%) or hydrogen abstraction (75%) at 298 K [*Barone et al.*, 1996; *Turnipseed et al.*, 1996], daytime oxidation of DMS by NO_3 may affect the yield of sulfate aerosol and thus the climate forcing due to marine sulfur emissions [e.g., *Lucas and Prinn*, 2005; Stark et al., submitted manuscript, 2006]. Highly reactive biogenic compounds, particularly α-pinene, were also oxidized to some extent by daytime NO_3 but were only observed in close proximity to their emission sources on the continent. An important consequence of NO_3-driven oxidation of continental biogenic VOCs are product yields (e.g., organic nitrates) that differ from OH or O_3 oxidation. This in turn may affect the O_3 forming potential of these VOCs [*Derwent et al.*, 2001] and/or the secondary organic aerosol (SOA) yields attributable to their oxidation [*Bonn and Moortgat*, 2002; *Chen and Griffin*, 2005; *Moldanova and Ljungstrom*, 2000]. Finally, although daytime NO_3-initiated oxidation was negligible for most anthropogenic VOCs, the calculated daytime oxidation rates of highly reactive anthropogenic VOCs (e.g., styrene, phenols) were enhanced by the presence of NO_3. Phenol is formed in high yield from OH oxidation of benzene [*Berndt and Böge*, 2006], and the subsequent oxidation of phenol by NO_3 could be a source of nitrated aromatics [*Harrison et al.*, 2005].

5.2. Heterogeneous NO_3 and N_2O_5 Chemistry in the Daytime

[23] Hydrolysis of N_2O_5 on aerosol (reaction (6)) is known as a major nighttime NO_x loss pathway, producing nitric acid and/or aerosol nitrate [*Brown et al.*, 2004], and heterogeneous uptake of NO_3 (reaction (7)) can initiate radical chemistry within particles [*Feingold et al.*, 2002; *Rudich et al.*, 1998]. Furthermore, production of nitryl chloride ($ClNO_2$) from heterogeneous N_2O_5 uptake on sea salt aerosol ($\gamma_{N_2O_5} = 3 \times 10^{-2}$ [*Hoffman et al.*, 2003]) followed by photolysis has been shown in laboratory studies to be a potential source of active halogens in the marine boundary layer [e.g., *Thornton and Abbatt*, 2005, and references therein]. It is therefore of interest to quantify heterogeneous reactions of NO_3 and N_2O_5 during the day.

5.2.1. Halogen Activation on Sea Salt

[24] The $ClNO_2$ production rate from heterogeneous N_2O_5 uptake can be estimated from the calculated steady state N_2O_5 concentration and the sea salt surface area,

Table 2. Representative Mixing Ratios of Oxidants and Calculated Fractions of VOCs Oxidized by NO_3 as a Function of NO_3 Photolysis Rate[a]

Molecule	$j(NO_3) > 0.18$ s^{-1}, e.g., 1000–1400 LT, No Cloud	0.08 $s^{-1} < j(NO_3) < 0.12$ s^{-1}, e.g., 0800, 1600, or Noon LT, Scattered Clouds	0.04 $s^{-1} < j(NO_3) < 0.06$ s^{-1}, e.g., 0600, 1800, or Noon LT, Dark Clouds
NO_x, ppbv	3.8	4.7	3.0
NO_3, pptv	0.06	0.14	0.24
OH, pptv	0.10	0.09	0.04
O_3, ppbv	46	39	39
f_{NO_3} (DMS)	11%	24%	53%
f_{NO_3} (α-pinene)	3.8%	9.7%	21%
f_{NO_3} (isoprene)	0.4%	1.0%	3.3%
f_{NO_3} (3-methyl furan)	7.1%	17%	39%
f_{NO_3} (styrene)	2.4%	6.1%	17%
f_{NO_3} (o-cresol)	9.7%	22%	50%
f_{NO_3} (phenol)	11%	25%	54%

[a]The value of $j(NO_3) > 0.18$ s^{-1} corresponds to clear sky, overhead sun, the value of (0.10 ± 0.02) s^{-1} to morning, afternoon, or partly cloudy conditions, and the value of (0.05 ± 0.01) s^{-1} to the period 1 hour after sunrise or 1 hour before sunset, or to cloudy conditions.

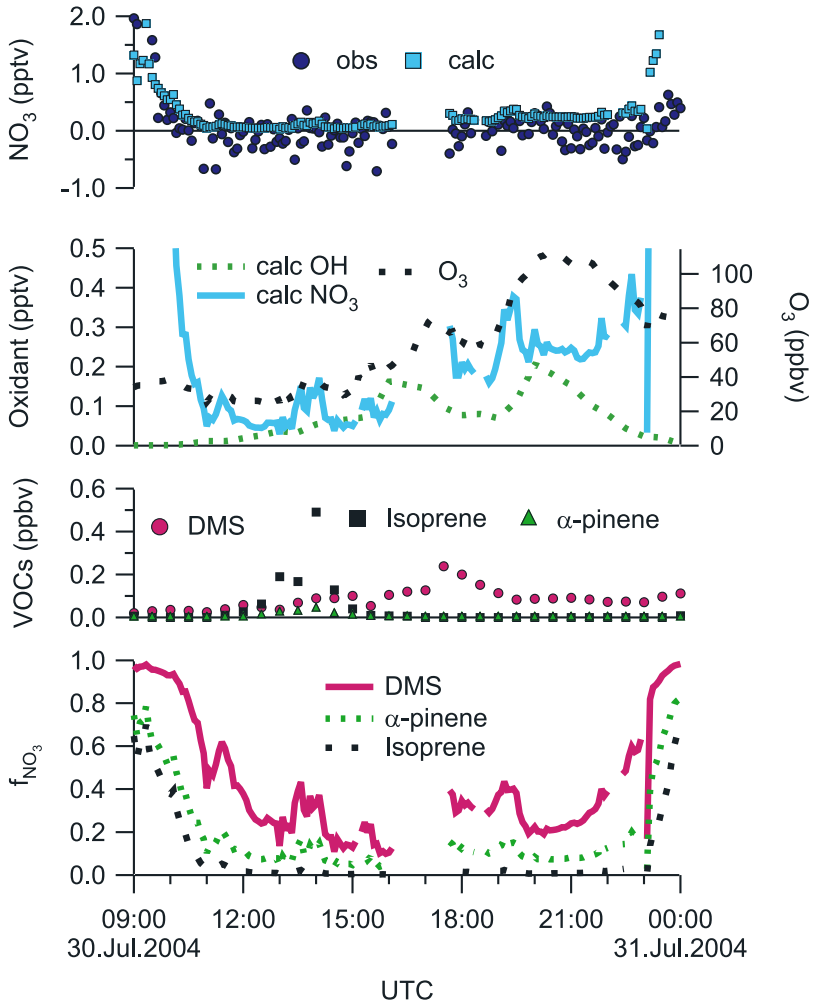

Figure 4. Calculated oxidation of volatile organic compounds in the marine boundary layer on 30 July 2004. The first panel shows comparison of calculated (equation (8)) with observed NO_3, which was within the uncertainty of baseline offsets (see text). The steady state calculation predicted 0.1–0.3 pptv of NO_3, consistent with the observed mixing ratio of N_2O_5 (Figure 3). The second panel shows time series of calculated OH, calculated NO_3, and measured O_3. Ambient OH levels were calculated using the Master Chemical Mechanism. The third panel shows observed mixing ratios of DMS, isoprene, and α-pinene. The fourth panel shows fraction of selected VOCs oxidized by NO_3 (equation (10)). At 1800 UTC (1400 LT) about 40% of DMS and about 15% of α-pinene were calculated to have been processed by NO_3. Oxidation of isoprene by NO_3 at daytime was calculated to be negligible.

derived from the number concentration of supermicron particles (measured with an aerodynamic particle sizer (APS) at 65% RH and corrected using growth factors given by *Tang et al.* [1997]), which were predominantly sea salt [*Bates et al.*, 2005]. The supermicron surface area density varied between 0.5 to 450 $\mu m^2\ cm^{-3}$ (average 33 $\mu m^2\ cm^{-3}$, median 22 $\mu m^2\ cm^{-3}$). A branching ratio, χ, for $ClNO_2$ production from N_2O_5 heterogeneous uptake may be defined such that the rate of $ClNO_2$ production is approximately $\chi k_6[N_2O_5]$.

$$\frac{d}{dt}[ClNO_2] = \chi k_6[N_2O_5], \left(\chi = \frac{\text{Area}(>1\mu)}{\text{Total Area}}\right) \qquad (11)$$

[25] The parameter χ was corrected for gas-phase diffusion [*Lovejoy and Hanson*, 1995] (average correction = 12%). On average, approximately 9% of the heterogeneous N_2O_5 uptake was predicted to have resulted in $ClNO_2$ generation. The average calculated $ClNO_2$, and thus chlorine, production rate from daytime N_2O_5 hydrolysis on sea salt was $\sim 9 \times 10^2$ molecules $cm^{-3}\ s^{-1}$ (1 pptv in 8 hours). Daytime uptake of N_2O_5 on sea salt aerosol could thus have been a continuous but small (compared to other sources such as the reaction of HCl with OH) source of chlorine.

5.2.2. Enhancement of Heterogeneous Uptake in Fog

[26] In the Gulf of Maine in the summer of 2004 the relative humidity of air was frequently near 100%, and fog was often encountered. In fog, concentrations of NO_3 and N_2O_5 (day or night) were below the instrumental detection limit, consistent with rapid heterogeneous uptake (e.g., $k_6 > 5 \times 10^{-3}\ s^{-1}$). Fog droplets have a very large surface area

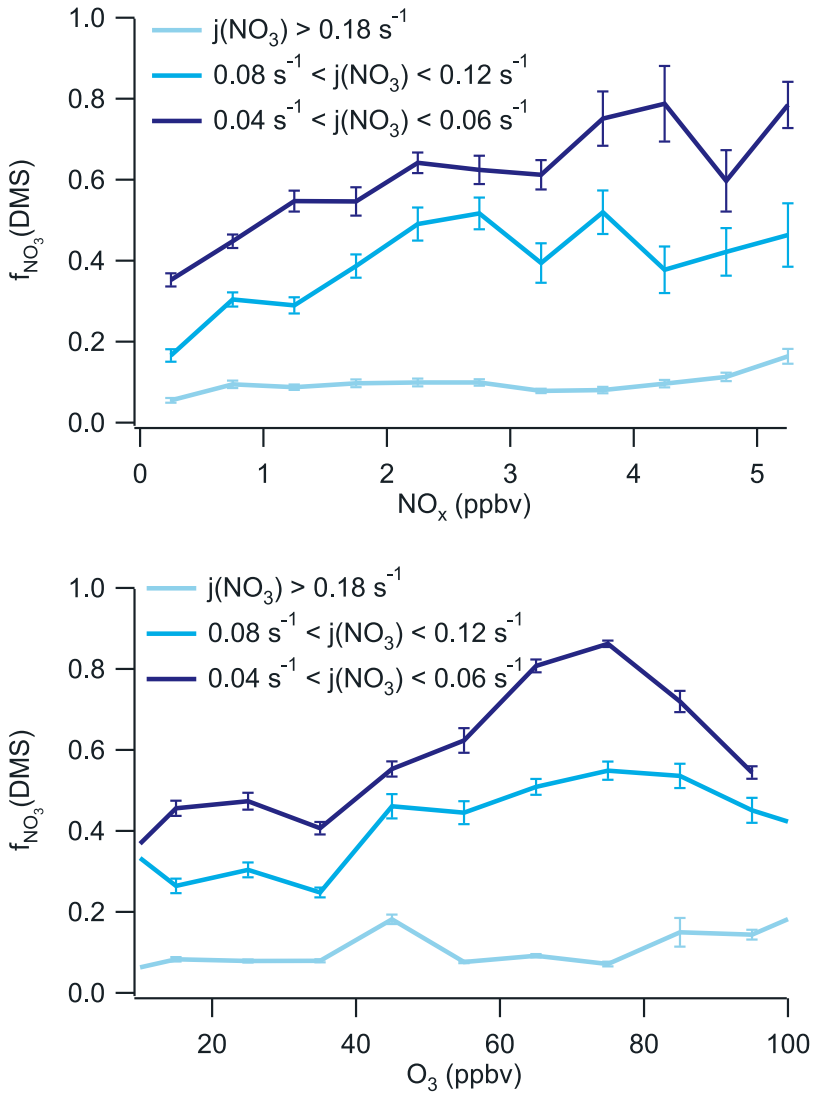

Figure 5. (top) Fraction of DMS oxidized by NO_3, relative to OH, binned by NO_x mixing ratio and averaged over the NEAQS-ITCT 2004 campaign. At NO_3 photolysis rates > 0.18 s^{-1} (i.e., midday, 1000–1400 LT), f_{NO_3} (DMS) is only weakly dependent on NO_x concentration, partly because NO_x-catalyzed production of O_3 and thus OH as well as higher ratios of photochemically produced NO relative to NO_2 compensate for higher rates of NO_3 production via reaction (1). At reduced photolysis rates, f_{NO_3} (DMS) scales more strongly with NO_x, because rates of photochemical OH production are reduced and the NO:NO_2 ratio is more favorable for NO_3 formation (i.e., NO:NO_2 ratio is smaller). (bottom) Fraction of DMS oxidized by NO_3, relative to OH, binned by O_3 mixing ratio and averaged over the NEAQS-ITCT 2004 campaign.

density and can therefore enhance heterogeneous reaction rates analogous to heterogeneous processing in clouds [*Lelieveld and Crutzen*, 1990]. Diffusion corrected loss rate coefficients of N_2O_5 and NO_3 on fog particles were calculated using a rough estimate of the fog droplet surface area density calculated from data of the aerosol extinction cavity ring-down spectrometer (T. Baynard et al., Design and application of a pulsed cavity ring-down aerosol extinction spectrometer for field measurements, submitted to *Aerosol Science and Technology*, 2006) and assuming uptake coefficients of N_2O_5 and NO_3 equal to those on pure water droplets ($\gamma_{N_2O_5}$ = 0.04, γ_{NO_3} = 2 × 10^{-4}) [*Rudich et al.*, 1996; *Vandoren et al.*, 1990]. Typical values of first-order loss rate coefficients of N_2O_5 and NO_3 on fog droplets were $k_6 \approx k_{fog}(N_2O_5) = 0.27\ s^{-1}$ and $k_7 \approx k_{fog}(NO_3) = 5.3 \times 10^{-3}\ s^{-1}$. Thus the calculated rate of N_2O_5 uptake on fog particles is larger than the rate of N_2O_5 thermal decomposition (k_{-2}(298K) = 0.038 s^{-1}, k_{-2}(288K) = 0.011 s^{-1}) [*Sander et al.*, 2003]. In fog, NO_3 and N_2O_5 were therefore likely not in equilibrium but in steady state. The ratio of N_2O_5:NO_3 is then

$$\frac{[N_2O_5]}{[NO_3]} \approx \frac{k_2[NO_2]}{k_{-2} + k_6}. \quad (12)$$

[27] The calculated rate of heterogeneous uptake of NO_3 in fog ($5.3 \times 10^{-3}\ s^{-1}$) was competitive with photolysis and reaction with NO. Any NO_3 taken up in the liquid phase

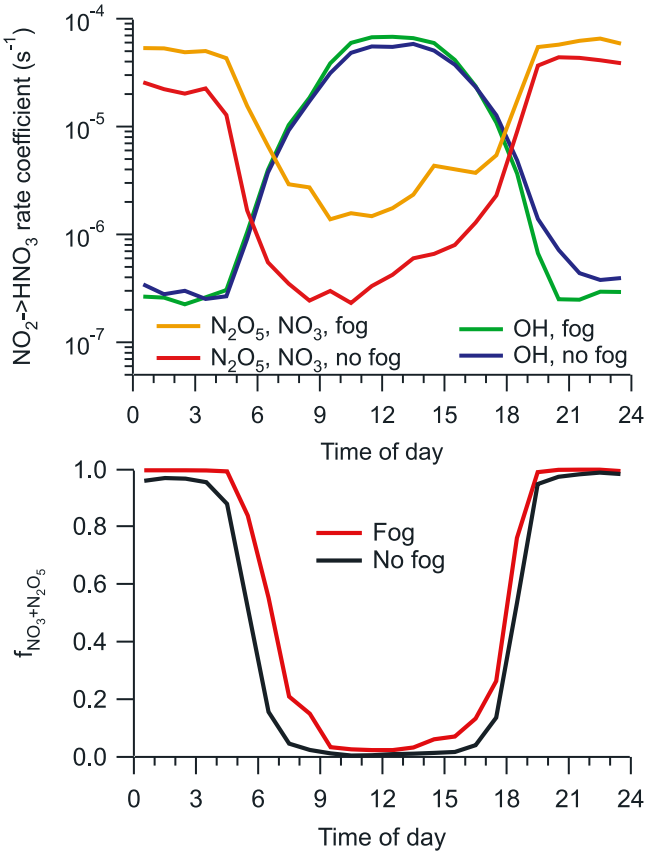

Figure 6. (top) Campaign-averaged calculated $NO_2 \rightarrow HNO_3$ conversion rate coefficients during NEAQS-ITCT 2004, plotted in fog and nonfog conditions. The daytime loss via $OH+NO_2$ (reaction (13)) was not significantly affected by fog, since photolysis rates were not attenuated. In contrast, daytime N_2O_5 hydrolysis was accelerated in fog. (bottom) Fraction of $NO_2 \rightarrow HNO_3$ conversion due to NO_3 and N_2O_5 chemistry.

likely converted to nitrate anion, for example by electron transfer reactions to Cl^-, Br^-, or SO_3^{2-}, which has been predicted to contribute to catalytic sulfur oxidation in the particle phase and release of halogens such as Br_2, BrCl, and Cl_2 into the gas phase [*Feingold et al.*, 2002; *Rudich et al.*, 1998]. The combined loss rate of NO_3 in fog ($\sim$0.02 s^{-1} in this example) was calculated to be within 10% of the maximum NO_3 photolysis rate ($j(NO_3)_{max} \approx 0.2\ s^{-1}$) and thus should have been nonnegligible during daytime.

5.2.3. Daytime NO_x to HNO_3 and Aerosol Nitrate Conversion

[28] The main photochemical source of HNO_3 is the reaction of NO_2 with OH.

$$NO_2 + OH \xrightarrow{M} HNO_3, k_{13} \tag{13}$$

The conversion rate of NO_2 to HNO_3 (including aerosol nitrate) in the marine boundary layer is approximately

$$\frac{d[HNO_3]}{dt} \approx k_{13}[NO_2][OH] + (\phi_5 k_5 + k_7)[NO_3] + (2-\chi)k_6[N_2O_5]. \tag{14}$$

[29] The parameter ϕ_5 accounts for the fractional yield of HNO_3 from VOC oxidation by NO_3 (e.g., 1 for DMS [*Jensen et al.*, 1992] and 0 for α-pinene [*Wangberg et al.*, 1997]), and $(2-\chi)$ accounts for $ClNO_2$ production, which upon photolysis recycles NO_2. Potential loss of NO_x via alkylnitrate, PAN, or pernitric acid (HNO_4) production [e.g., *Stroud et al.*, 2003] has been neglected in this analysis. DMS and aldehydes were the only VOCs sufficiently abundant to yield significant amounts of HNO_3. Heterogeneous uptake of NO_3 (reaction (7)) was significant in fog only (section 5.2.2). To determine the amount of HNO_3 produced by daytime NO_3 and N_2O_5 reactions, it is convenient to define a parameter ϕ_{HNO_3} so that the amount of HNO_3 and aerosol nitrate produced by NO_3 and N_2O_5 reactions can be calculated by multiplying ϕ_{HNO_3} with the NO_3 production rate:

$$\phi_{HNO_3} = \frac{(2-\chi)k_6\left(\frac{k_2[NO_2]}{k_{-2}+k_6}\right) + \phi_5 k_5 + k_7}{k_3[NO] + j_4 + k_5 + k_6\left(\frac{k_2[NO_2]}{k_{-2}+k_6}\right) + k_7} \tag{15}$$

$$\frac{d[HNO_3]}{dt} \approx \left(k_{13}[OH]_{calc} + \phi_{HNO_3} k_1[O_3]\right)[NO_2] \tag{16}$$

[30] In the absence of fog, the average noontime value of the parameter $\phi_{HNO_3}$was 0.02; that is, 98% of the NO_3 produced via reaction (1) was destroyed via reactions that do not produce HNO_3 (e.g., reactions (3) or (4)). In fog at noon, the average value of ϕ_{HNO_3} was 0.11. In this case, the numerator of equation (15) was dominated by heterogeneous uptake of N_2O_5 and NO_3.

[31] Shown in Figure 6 are campaign averaged first-order rate coefficients for conversion of NO_2 to HNO_3 plotted as a function of time of day in fog and nonfog conditions. The photolytic production of OH and thus the reaction rate of NO_2 with OH (reaction (13)) were not affected by fog because the fog layers encountered during this campaign were shallow and tended to diffuse, but not attenuate, the sunlight. The average daytime HNO_3 and aerosol nitrate production rate coefficient from NO_3 and N_2O_5 was approximately 30$\times$ larger in the presence of fog. As a result, the nocturnal dominance of heterogeneous NO_3 and N_2O_5 uptake as HNO_3 production route extended 1 hour into the morning and late afternoon (Figure 6, bottom).

[32] As noted above, the calculated nitric acid production from daytime NO_3 and N_2O_5, averaged from 0900 to 1500 LT, was only about 2% relative to $OH + NO_2$, but averaged 5% in the presence of fog. The relatively small contribution of NO_3 and N_2O_5 to daytime nitric acid production in fog was due to the consistently small NO_2 concentrations (median $\sim$520 pptv, > 90% of the data points < 1 ppbv), which in turn were likely a consequence of the geographic distribution of fog toward the northeast end of the study area, well away from coastal NO_x emission sources. Small NO_2 concentrations shift the equilibrium between NO_3 and N_2O_5 toward NO_3, which has a much smaller uptake coefficient than N_2O_5.

[33] Shown in Figure 7 (middle) is a histogram of calculated nitric acid yield from daytime NO_3 and N_2O_5

in fog as a function of NO_2 mixing ratio. The rates of heterogeneous NO_3 and N_2O_5 uptake in fog scale with NO_2 concentration (Figure 7, middle). Furthermore, the fraction of nitric acid produced from daytime NO_3 and N_2O_5 relative to OH increases significantly with NO_2 concentration (Figure 7, bottom). Thus, in polluted fog (i.e., > 5 ppbv NO_2) heterogeneous NO_3 and N_2O_5 uptake is calculated to be competitive with OH + NO_2 as a daytime NO_x loss process. Although these daytime heterogeneous reactions had little effect on average in this data set, they could be a considerable daytime NO_x (and O_3) destruction mechanism under highly polluted, NO_x-rich conditions where heterogeneous processes are rapid (e.g., in haze or fog).

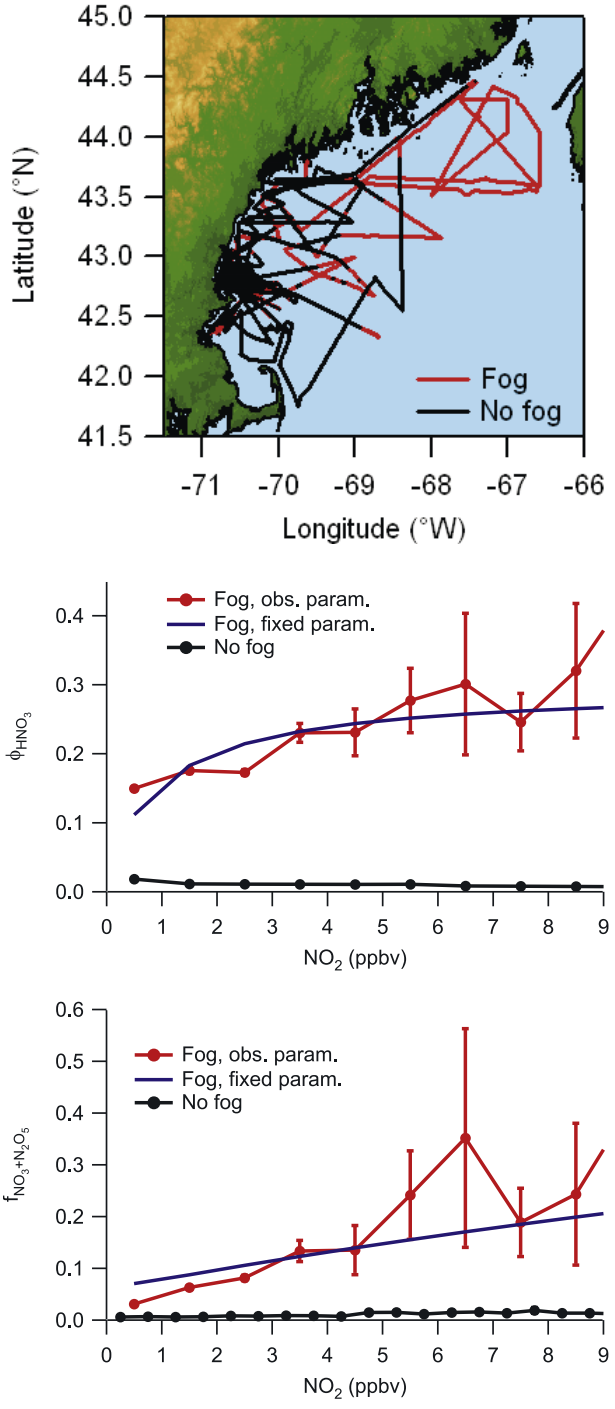

Figure 7. (top) Geographical distribution of daytime ship locations in the presence and absence of fog. (middle) Daytime yield of HNO_3 and aerosol nitrate, ϕ_{HNO_3}, from NO_3 and N_2O_5, binned by NO_2 concentration. Error bars are $\pm 1\sigma$. In fog, the calculated yield of HNO_3 from heterogeneous NO_3 and N_2O_5 uptake scales with NO_2 concentration. The median NO_2 concentration in daytime fog was 520 pptv. The smooth trace was calculated with O_3 = 50 ppbv, $j(NO_2) = 6.1 \times 10^{-3}$ s^{-1}, $j_4 = 0.2$ s^{-1}, $k_5 = 0$ s^{-1}, $k_6 = 0.27$ s^{-1}, and $k_7 = 5.3 \times 10^{-3}$ s^{-1}. Concentrations of NO were calculated assuming a photostationary state [*Leighton*, 1961]. (bottom) Fraction of HNO_3 produced via daytime NO_3 and N_2O_5 reactions relative to reaction (13), i.e., OH + NO_2, $\left(\frac{k_1\phi_{HNO_3}[O_3]}{k_1\phi_{HNO_3}[O_3]+k_{14}[OH]}\right)$ binned by NO_2 concentration. The smooth trace was calculated with the same parameters as above and OH concentrations calculated from the Ehhalt parameterization [*Ehhalt and Rohrer*, 2000]. At NO_2 concentrations greater than 5 ppbv in daytime fog, more than 15% of HNO_3 are calculated to be generated from NO_3 and N_2O_5 heterogeneous uptake.

5.3. Daytime O_x Destruction and Leighton Ratio Perturbation

[34] Reactions of NO_3 and N_2O_5 enhance the loss rate of odd oxygen, or O_x (= $NO_2 + O_3 + 2NO_3 + 3N_2O_5$) [*Brown et al.*, 2006; *Wood et al.*, 2005] during the day. For example, photolysis of NO_3 to NO (reaction (4b)) destroys ozone in a catalytic cycle [*Brown et al.*, 2005] with rate

$$\frac{d[O_3]}{dt} = -2j_{4b}[NO_3]_{calc}. \quad (17)$$

In addition to this photolytic pathway, O_x is consumed by gas phase reactions of NO_3 with VOCs and heterogeneous reactions of N_2O_5 and NO_3 [*Brown et al.*, 2005].

[35] Overall, the impact of daytime NO_3 and N_2O_5 reactions on O_x loss was small for the R/V *Brown* NEAQS-ITCT data set, with an average, integrated midday (0900–1500 LT, solar zenith angle < 45°) loss of 152 pptv, and an average, noontime loss rate of 20 pptv h^{-1} (26 pptv h^{-1} in fog). These rates are inconsequential in comparison to surface deposition, estimated at 1.5 pbbv O_3 h^{-1} (deposition velocity of 0.1 cm s^{-1} [*Galbally and Roy*, 1980; *Gallagher et al.*, 2001] from a 100 m marine boundary layer depth). The calculated O_x loss rates are also substantially smaller than those inferred from a similar analysis of data from Houston, TX, in 2000 [*Geyer et al.*, 2003], largely because of the relatively lower O_3 and NO_2 concentrations.

[36] In the daytime, a photostationary state exists between NO and NO_2, in which NO_2 is produced by oxidation of NO with O_3 and destroyed by photolysis [*Leighton*, 1961]. This photostationary state can be perturbed by processes that enhance the NO oxidation rate, for example by reaction of NO with peroxy radicals such as HO_2 or RO_2 [e.g., *Volz-Thomas et al.*, 2003], or by the nitrate radical [*Brown et al.*, 2005; *Geyer et al.*, 2003].

[37] For this data set, the NO_2:NO ratio was calculated to have increased by up to 18% because of peroxy radical

Table 3. Calculated Perturbation of the NO_2:NO Ratio Due to Peroxy and Daytime NO_3 and N_2O_5 Chemistry, Calculated on the Basis of Input Parameters Typical for the NEAQS-ITCT 2004 Data Set in Nonfog Conditions[a]

	Morning (0600 LT)	Noon	Evening (1800 LT)
$[O_3]$, ppbv	30	44	52
$j(NO_2)$, 10^{-3} s^{-1}	1.2	6.2	1.2
$j(NO_3)$, 10^{-2} s^{-1}	5.4	18	5.4
$\Sigma[RO_2]$, pptv	4.7	9.8	6.4
$[HO_2]$, pptv	1.4	9.9	1.4
[NO], ppbv	0.49	0.51	0.09
k_5, 10^{-3} s^{-1}	6.7	4.9	5.7
k_6, 10^{-4} s^{-1}	6.0	6.3	6.7
$[NO_3]_{calc}$, pptv	0.40	0.14	0.69
$[N_2O_5]_{calc}$, pptv	1.79	0.20	0.97
NO_2:NO, photostationary state	11.88	3.37	20.58
NO_2:NO, peroxy radicals included	12.87	4.00	21.85
NO_2:NO, peroxy radicals and NO_3 included	13.08	4.01	22.22
% effect, peroxy radicals	+8.3%	+18.7%	+6.2%
% effect, NO_3 + NO (reaction (3))	+1.6%	+0.3%	+1.3%

[a]The "% effect" is the perturbation relative to the photostationary state expression [*Leighton*, 1961].

chemistry but was only marginally affected (up to 0.3% at noon) by NO_3 reactions (Table 3). Overall, perturbation of the NO_2:NO ratio by daytime NO_3 and N_2O_5 was only important during day-night transition periods or in fresh pollution plumes when the photostationary state approximation is of questionable accuracy because of the increased time required to achieve a steady state.

6. Conclusions

[38] Daytime N_2O_5 was observed in the summertime marine boundary layer at concentrations of up to 4 pptv. This observation implies the presence of NO_3, whose concentrations were estimated from known kinetic and equilibrium relationships. The presence of these compounds during the day enhances the oxidation rate of reactive VOCs, changes the product yield from VOC oxidation, and increases the conversion rate of NO_x to HNO_3, in particular in fog under conditions of high NO_x. Additional effects, such as the increased chemical destruction of odd oxygen (O_x) and perturbation of the Leighton photostationary state, were calculated to have been modest.

[39] There are indications in this data set that the role of daytime NO_3 and N_2O_5 is significantly enhanced in low-light conditions, for example under cloud cover, during the periods close to sunset and sunrise, as well as in highly polluted, i.e., NO_x- and O_3-rich, plumes. Furthermore, daytime NO_3 and N_2O_5 reactions are expected to be of somewhat greater importance in other seasons, when greater solar zenith angles reduce the photolytic loss of NO_3, the ratio of NO:NO_2, and, thus, the losses of NO_3 via reaction (3). In addition, the greater partitioning of NO_3 to N_2O_5 at colder temperatures should enhance the importance of heterogeneous N_2O_5 processes.

[40] **Acknowledgments.** The authors thank the crew and fellow scientists on board R/V *Brown* during NEAQS-ITCT 2004. Funding was provided in part by NOAA's Air Quality program and in part by NOAA's Climate Forcing program.

References

Aldener, M., et al. (2006), Reactivity and loss mechanisms of NO_3 and N_2O_5 in a polluted marine environment: Results from in situ measurements during New England Air Quality Study 2002, *J. Geophys. Res.*, doi:10.1029/2006JD007252, in press.

Atkinson, R. (1990), Gas-phase tropospheric chemistry of organic-compounds—A review, *Atmos. Environ., Part A*, *24*, 1–41.

Atkinson, R. (1991), Kinetics and mechanisms of the gas-phase reactions of the NO_3 radical with organic-compounds, *J. Phys. Chem. Ref. Data*, *20*, 459–507.

Atkinson, R., and J. Arey (2003), Atmospheric degradation of volatile organic compounds, *Chem. Rev.*, *103*, 4605–4638.

Atkinson, R., et al. (1999), Evaluated kinetic and photochemical data for atmospheric chemistry, organic species: Supplement VII, *J. Phys. Chem. Ref. Data*, *28*, 191–393.

Barone, S. B., et al. (1996), Reaction of OH with dimethyl sulfide (DMS). 1. Equilibrium constant for OH + DMS reaction and the kinetics of the OH center dot DMS + O_2 reaction, *J. Phys. Chem.*, *100*, 14,694–14,702.

Bates, T. S., et al. (2005), Dominance of organic aerosols in the marine boundary layer over the Gulf of Maine during NEAQS 2002 and their role in aerosol light scattering, *J. Geophys. Res.*, *110*, D18202, doi:10.1029/2005JD005797.

Berndt, T., and O. Böge (2006), Formation of phenol and carbonyls from the atmospheric reaction of OH radicals with benzene, *Phys. Chem. Chem. Phys.*, *8*(10), 1205–1214.

Bonn, B., and G. K. Moortgat (2002), New particle formation during alpha- and beta-pinene oxidation by O_3, OH and NO_3, and the influence of water vapour: Particle size distribution studies, *Atmos. Chem. Phys.*, *2*, 183–196.

Brown, S. S., et al. (2004), Nighttime removal of NO_x in the summer marine boundary layer, *Geophys. Res. Lett.*, *31*, L07108, doi:10.1029/2004GL019412.

Brown, S. S., et al. (2005), Aircraft observations of daytime NO_3 and N_2O_5 and their implications for tropospheric chemistry, *J. Photochem. Photobiol. A Chem.*, *176*, 270–278.

Brown, S. S., et al. (2006), Nocturnal odd-oxygen budget and its implications for ozone loss in the lower troposphere, *Geophys. Res. Lett.*, *33*, L08801, doi:10.1029/2006GL025900.

Butkovskaya, N. I., and G. Lebras (1994), Mechanism of the NO_3 + DMS reaction by discharge flow mass-spectrometry, *J. Phys. Chem.*, *98*, 2582–2591.

Carslaw, N., et al. (1999a), Modeling OH, HO_2, and RO_2 radicals in the marine boundary layer: 1. Model construction and comparison with field measurements, *J. Geophys. Res.*, *104*, 30,241–30,255.

Carslaw, N., et al. (1999b), Modeling OH, HO_2, and RO_2 radicals in the marine boundary layer: 2. Mechanism reduction and uncertainty analysis, *J. Geophys. Res.*, *104*, 30,257–30,273.

Chen, J. J., and R. J. Griffin (2005), Modeling secondary organic aerosol formation from oxidation of alpha-pinene, beta-pinene, and d-limonene, *Atmos. Environ.*, *39*, 7731–7744.

Crutzen, P. J. (1979), Role of NO and NO_2 in the chemistry of the troposphere and stratosphere, *Annu. Rev. Earth Planet. Sci.*, *7*, 443–472.

D'Anna, B., et al. (2001), Kinetic study of OH and NO_3 radical reactions with 14 aliphatic aldehydes, *Phys. Chem. Chem. Phys.*, *3*, 3057–3063.

de Gouw, J. A., et al. (2005), Budget of organic carbon in a polluted atmosphere: Results from the New England Air Quality Study in 2002, *J. Geophys. Res.*, *110*, D16305, doi:10.1029/2004JD005623.

Derwent, R. G., et al. (2001), Characterization of the reactivities of volatile organic compounds using a master chemical mechanism, *J. Air Waste Manage. Assoc.*, *51*, 699–707.

Dubé, W. P., et al. (2006), Aircraft instrument for simultaneous, in situ measurement of NO_3 and N_2O_5 via pulsed cavity ring-down spectroscopy, *Rev. Sci. Instrum.*, *77*, 034101.

Ehhalt, D. H., and F. Rohrer (2000), Dependence of the OH concentration on solar UV, *J. Geophys. Res.*, *105*, 3565–3572.

Fehsenfeld, F. C., et al. (2006), International Consortium for Atmospheric Research on Transport and Transformation (ICARTT): North America to Europe—Overview of the 2004 summer field study, *J. Geophys. Res.*, doi:10.1029/2006JD007829, in press.

Feingold, G., G. J. Frost, and A. R. Ravishankara (2002), Role of NO_3 in sulfate production in the wintertime northern latitudes, *J. Geophys. Res.*, *107*(D22), 4640, doi:10.1029/2002JD002288.

Galbally, I. E., and C. R. Roy (1980), Destruction of ozone at the Earth's surface, *Q. J. R. Meteorol. Soc.*, *106*, 599–620.

Gallagher, M. W., et al. (2001), Ozone deposition to coastal waters, *Q. J. R. Meteorol. Soc.*, *127*, 539–558.
Geyer, A., et al. (2003), Direct observations of daytime NO_3: Implications for urban boundary layer chemistry, *J. Geophys. Res.*, *108*(D12), 4368, doi:10.1029/2002JD002967.
Goldan, P. D., et al. (2004), Nonmethane hydrocarbon and oxyhydrocarbon measurements during the 2002 New England Air Quality Study, *J. Geophys. Res.*, *109*, D21309, doi:10.1029/2003JD004455.
Harrison, M. A. J., et al. (2005), Nitrated phenols in the atmosphere: A review, *Atmos. Environ.*, *39*, 231–248.
Hoffman, R. C., et al. (2003), Knudsen cell studies of the reactions of N_2O_5 and $ClONO_2$ with NaCl: Development and application of a model for estimating available surface areas and corrected uptake coefficients, *Phys. Chem. Chem. Phys.*, *5*, 1780–1789.
Hu, J. H., and J. P. D. Abbatt (1997), Reaction probabilities for N_2O_5 hydrolysis on sulfuric acid and ammonium sulfate aerosols at room temperature, *J. Phys. Chem. A*, *101*, 871–878.
Jenkin, M. E., et al. (2003), Protocol for the development of the Master Chemical Mechanism, MCM v3 (Part B): Tropospheric degradation of aromatic volatile organic compounds, *Atmos. Chem. Phys.*, *3*, 181–193.
Jensen, N. R., et al. (1992), Products and mechanisms of the gas-phase reactions of NO_3 with CH_3SCH_3, CD_3SCD_3, CH_3SH and CH_3SSCH_3, *J. Atmos. Chem.*, *14*, 95–108.
Johnston, H. S., et al. (1996), NO_3 photolysis product channels: Quantum yields from observed energy thresholds, *J. Phys. Chem.*, *100*, 4713–4723.
Leighton, P. A. (1961), *Photochemistry of Air Pollution*, Elsevier, New York.
Lelieveld, J., and P. J. Crutzen (1990), Influences of cloud photochemical processes on tropospheric ozone, *Nature*, *343*, 227–233.
Lovejoy, E. R., and D. R. Hanson (1995), Measurement of the kinetics of reactive uptake by submicron sulfuric-acid particles, *J. Phys. Chem.*, *99*, 2080–2087.
Lucas, D. D., and R. G. Prinn (2005), Sensitivities of gas-phase dimethylsulfide oxidation products to the assumed mechanisms in a chemical transport model, *J. Geophys. Res.*, *110*, D21312, doi:10.1029/2004JD005386.
Moldanova, J., and E. Ljungstrom (2000), Modelling of particle formation from NO_3 oxidation of selected monoterpenes, *J. Aerosol. Sci.*, *31*, 1317–1333.
Mozurkewich, M., and J. G. Calvert (1988), Reaction probability of N_2O_5 on aqueous aerosols, *J. Geophys. Res.*, *93*, 15,889–15,896.
Platt, U., and G. Honninger (2003), The role of halogen species in the troposphere, *Chemosphere*, *52*, 325–338.
Roberts, J. M., et al. (1984), Measurements of aromatic hydrocarbon ratios and NO_x concentrations in the rural troposphere—Observation of air-mass photochemical aging and NO_x removal, *Atmos. Environ.*, *18*, 2421–2432.
Roberts, J. M., et al. (1998), Measurements of PAN, PPN, and MPAN made during the 1994 and 1995 Nashville Intensives of the Southern Oxidant Study: Implications for regional ozone production from biogenic hydrocarbons, *J. Geophys. Res.*, *103*, 22,473–22,490.
Rudich, Y., et al. (1996), Reactive uptake of NO_3 on pure water and ionic solutions, *J. Geophys. Res.*, *101*, 21,023–21,031.
Rudich, Y., et al. (1998), Multiphase chemistry of NO_3 in the remote troposphere, *J. Geophys. Res.*, *103*, 16,133–16,143.
Sander, S. P. et al., (2003), *Chemical Kinetics and Photochemical Data for Use in Atmospheric Studies*, Jet Propul. Lab., Pasadena, Calif.
Saunders, S. M., et al. (2003), Protocol for the development of the Master Chemical Mechanism, MCM v3 (Part A): Tropospheric degradation of non-aromatic volatile organic compounds, *Atmos. Chem. Phys.*, *3*, 161–180.
Stohl, A., et al. (2005), Technical note: The Lagrangian particle dispersion model FLEXPART version 6.2, *Atmos. Chem. Phys.*, *5*, 2461–2474.
Stroud, C., et al. (2003), Photochemistry in the arctic free troposphere: NO_x budget and the role of odd nitrogen reservoir recycling, *Atmos. Environ.*, *37*, 3351–3364.
Tang, I. N., et al. (1997), Thermodynamic and optical properties of sea salt aerosols, *J. Geophys. Res.*, *102*, 23,269–23,275.
Thornton, J. A., and J. P. D. Abbatt (2005), N_2O_5 reaction on submicron sea salt aerosol: Kinetics, products, and the effect of surface active organics, *J. Phys. Chem. A*, *109*, 10,004–10,012.
Turnipseed, A. A., et al. (1996), Reaction of OH with dimethyl sulfide. 2. Products and mechanisms, *J. Phys. Chem.*, *100*, 14,703–14,713.
Vandoren, J. M., et al. (1990), Temperature-dependence of the uptake coefficients of HNO_3, HCl, and N_2O_5 by water droplets, *J. Phys. Chem.*, *94*, 3265–3269.
Voigt, S., et al. (2002), The temperature and pressure dependence of the absorption cross-sections of NO_2 in the 250–800 nm region measured by Fourier-transform spectroscopy, *J. Photochem. Photobiol. A Chem.*, *149*, 1–7.
Volz-Thomas, A., H. Pätz, N. Houben, S. Konrad, D. Mihelcic, T. Klüpfel, and D. Perner (2003), Inorganic trace gases and peroxy radicals during BERLIOZ at Pabstthum: An investigation of the photostationary state of NO_x and O_3, *J. Geophys. Res.*, *108*(D4), 8248, doi:10.1029/2001JD001255.
Wallington, T. J., et al. (1986), Absolute rate constants for the gas-phase reactions of the NO_3 radical with CH_3SH, CH_3SCH_3, CH_3SSCH_3, H_2S, SO_2, and CH_3OCH_3 over the temperature range 280K–350K, *J. Phys. Chem.*, *90*, 5393–5396.
Wangberg, I., et al. (1997), Product and mechanistic study of the reaction of NO_3 radicals with alpha-pinene, *Environ. Sci. Technol.*, *31*, 2130–2135.
Wayne, R. P., et al. (1991), The nitrate radical—Physics, chemistry, and the atmosphere, *Atmos. Environ., Part A*, *25*, 1–203.
Williams, E. J., et al. (1998), Intercomparison of ground-based NO_y measurement techniques, *J. Geophys. Res.*, *103*, 22,261–22,280.
Wood, E. C., et al. (2005), Measurements of N_2O_5, NO_2, and O_3 east of the San Francisco Bay, *Atmos. Chem. Phys.*, *5*, 483–491.
Yokelson, R. J., et al. (1994), Temperature-dependence of the NO_3 absorption-spectrum, *J. Phys. Chem.*, *98*, 13,144–13,150.

T. S. Bates and D. Coffman, Pacific Marine Environmental Laboratory, NOAA, 7600 Sand Point Way NE, Seattle, WA 98115, USA.

T. Baynard, S. Brown, P. D. Goldan, W. C. Kuster, B. M. Lerner, S. H. D. Osthoff, A. Pettersson, A. R. Ravishankara, J. M. Roberts, R. Sommariva, H. Stark, and E. J. Williams, Chemical Sciences Division, Earth System Research Laboratory, NOAA, 325 Broadway, Boulder, CO 80305, USA. (steven.s.brown@noaa.gov)